Pontificia Universidad
JAVERIANA
Bogotá

Univ. Sci. 28(3): 316–335, 2023
doi: 10.11144/Javeriana.SC283.sona

ORIGINAL ARTICLE

# Study of $NiO/Al_2O_3$ and $NiO/Zn\text{-}Al_2O_3$ catalysts for water gas shift reaction

**Edgardo Meza-Fuentes***[1], **Johana Rodriguez-Ruiz**[1,2], **Edinson Castellar-Arroyo**[1], **Maria do Carmo Rangel**[3], **Eduardo Espinosa-Fuentes**[4]

**Edited by**
Angela Johana Espejo Mojica
editorus@javeriana.edu.co

**1**. Grupo de Estudios en Materiales y Combustibles, Campus San Pablo, Universidad de Cartagena, Cartagena, Colombia.

**2**. Grupo de Investigación en Procesos de la Industria Petroquímica, SENA-Centro para la Industria Petroquímica, Cartagena, Colombia.

**3**. Instituto de Química, Universidade Federal do Rio Grande do Sul. Av. Bento Gonçalves, 9500, Agronomia, 90650-001 Porto Alegre, RS, Brazil.

**4**. Universidad Libre, Km. 7, Vía Antigua Puerto Colombia, Barranquilla, Colombia.

*emezaf@unicartagena.edu.co

**Received:** 24-05-2023
**Accepted:** 08-11-2023
**Published online:** 12-12-2023

**Citation:** Meza-fuentes E, Rodríguez-Ruiz J, Castellar-Arroyo E, Rangel M, Espinosa-Fuentes E. Study of NiO/Al2O3 and NiO/Zn-Al2O3 catalysts for water gas shift reaction, *Universitas Scientiarum*, 28(3): 300–315, 2023. doi: 10.11144/Javeriana.SC283.sona

**Funding:** n.a.

**Electronic supplementary material:** n.a.

## Abstract

Nickel-based catalysts are of great importance for the generation of hydrogen from natural gas. Within this process, the conditions in which commercial $NiO/Al_2O_3$ is converted to $Ni^0/Al_2O_3$ catalyst should be further investigated. A widely used technique to identify $Ni^{2+}$ reduction conditions and the different compounds or types of particles in which this element is present is temperature-programmed reduction. In this work, the type of nickel oxide particles occurring on $Al_2O_3$ and $ZnO\text{-}Al_2O_3$-based supports were studied by different techniques, such as energy-dispersive X-ray spectroscopy, FTIR, the BET method, X-ray diffraction (XRD), and Temperature Programmed Reduction (TPR). All materials were evaluated in the water gas shift reaction (WGS), and the influence of their characteristics on the catalytic activity was assessed. Solids were prepared at different temperatures and Ni/Zn molar ratios. The results showed the presence of NiO in all materials, as well as the presence of ZnO, $NiAl_2O_4$, and $ZnAl_2O_4$ in materials prepared at higher temperatures. In all the materials calcined at the lowest temperature, the formation of NiO particles that fail to interact with the supports was prioritized. As the calcination temperature increased, NiO aggregates were formed, which, to a greater degree, interacted with the supports, whereby nickel aluminate was detected in all materials prepared at 750 °C. Zinc increased the selectivity but decreased specific surface area and activity through the WGS reaction. The solid labeled AZ15-500 showed higher activity and selectivity, reaching values of 100% for the water gas shift reaction.

**Keywords:** catalysis; NiO particles; temperature programmed reduction; temperature effect; water gas shift reaction

## 1. Introduction

Catalysis is one of chemistry's tenants; it enables and accelerates key reactions, which could not have been possible by ordinary synthesis methods because of their unselectivity and low yields. Catalysts have, therefore, revolutionized and promoted industrial and research development. Many catalysts are made up of salts, oxides, or other types of compounds. One of the simplest analysis techniques for catalyst characterization is temperature-programmed reduction (TPR). TPR has a wide range of applications to determine the reduction conditions of metallic species that occur in compounds such as oxides, sulfides, and nitrates, among others [1, 2, 3, 4, 5, 6, 7]. TPR's main application is in research and industrial fields with a focus on heterogeneous catalysis, the processes by which metal catalysts derive from precursors in the form of oxides or other types of inorganic compounds [1, 2, 3, 4, 5, 6, 7, 8, 9].

Reduction studies are generally carried out in setups where the solids to be analyzed are subjected to certain heating rates in the presence of a reducing gas such as hydrogen, mixed with an inert gas, such as nitrogen or argon, in a greater proportion [1, 2, 3, 4, 5, 6, 7, 8, 9, 10, 11]. In many cases the solids to be studied are oxides, so the analytic equipment includes a section wherein the water produced during the reduction process is collected in traps based on zeolites or in a cooling system based on a mixture of liquid nitrogen with alcohols such as ethylene glycol. The determination of the hydrogen spent as a function of the temperature or the time at which the reaction occurs is usually carried out with thermal conductivity detectors (TCD) and flame ionization detectors (FID). Thermogravimetric Analysis (TGA) equipment can also be used, whereby the reduction temperature is determined by mass loss [10].

In catalysis, one of the main applications of TPR lies in the study of nickel oxide (NiO) particles supported on aluminum oxides. These systems are used in the industrial field as catalysts within reactions to obtain hydrogen through methane reforming, water gas shift reaction (WGSR), and methane reforming with carbon dioxide [10, 12, 13, 14, 15]. NiO reduction to metallic nickel ($Ni^0$) has been extensively studied by TPR since the late 20th century and the concepts described are still valid [16, 17]. During this process, the reduction of part of the NiO on the surface of the particles occurs first, followed by a second reduction in the interface between the NiO and the previously formed $Ni^0$. At this stage, an autocatalytic process is induced, which extends throughout the formation of $Ni^0$ nuclei and is then slowed down by the formation of water molecules that decrease the reaction.

Generally, during NiO reduction with hydrogen, the oxide begins to be reduced by forming clusters that spread on a two-dimensional basis along the surface until they overlap each other. During this step, the hydrogen dissociates on Ni atoms, which allows its diffusion into particles, leading to the advancement of the reaction [11, 18, 19].

In TPR analyses, NiO originates a single reduction peak, which is recorded at temperatures that chiefly depend on the synthesis method and particle size and morphology [17, 18, 20, 21]. In the industrial field and in heterogeneous catalysis, nickel oxide is commonly marketed in the form of oxide particles supported on alumina ($NiO\text{-}Al_2O_3$), thereby, a greater specific surface area is exhibited NiO particles disperse broadly, which increases their catalytic activity. This type of catalyst can be prepared by different methods, such as the impregnation of solutions containing $Ni^{2+}$ in aluminum oxides, or by means of simultaneous coprecipitation of metal hydroxides, followed by calcination processes to generate the respective metal oxides [1, 2, 8, 9, 10, 22]. The study of NiO particles in this type of solids with X-ray diffraction is challenging due to the presence of amorphous phases characteristic of alumina-type compounds, which originate diffractograms with wide and asymmetric peaks that hinder the identification of peaks corresponding to NiO. In this context, the TPR technique is preferred to identify the different types of NiO particles supported in aluminum oxides and silicon, among other materials, generated through the various synthesis methods [23, 24, 25, 26].

NiO particles can cause reduction peaks at different temperatures, which depend on the type of interaction that they develop with the support. In this sense, Scheffert and collaborators [16] carried out several research efforts that allowed for the identification of the degree of interaction between NiO and aluminum oxides as a function of the recording temperature of reduction peaks by TPR, thus concluding that: a) NiO particles without interaction with the support originate peaks at temperatures lower than 327 °C; b) particles with weak, intermediate and strong interactions with the support produce peaks between 327 and 727 °C; and c) $NiAl_2O_4$ particles produce peaks at temperatures above 750 °C.

In previous studies, we observed that in materials based on NiO/ZnO/$Al_2O_3$ obtained from hydrotalcite, the presence of ZnO decreases the incorporation of $Al^{3+}$ cations in the cubic crystalline lattice of NiO, which leads to an increase in the selectivity of these materials for the WGS reaction [1, 2]. Likewise, ZnO favors the formation of NiO particles that do not interact with the $Al_2O_3$-based support [1, 2]. In the present work, solids based on nickel-aluminum and nickel-zinc-aluminum were synthesized and studied by different techniques, mainly TPR, XRD, EDX, BET, and FTIR. Thanks to these techniques we observed of the types of NiO particles formed, identified of influence of ZnO on the types of NiO particles formed, and studied how they affect the catalytic activity for the WGS reaction.

## 2. Materials and Methods

### 2.1. Materials preparation

For the preparation of compound solids based on nickel-aluminum (Ni-Al), 150 mL of individual solutions of $Ni(NO_3)_2$ $6H_2O$ and $Al(NO_3)_3$ $9H_2O$ were prepared in the Ni/Al=0.5 molar ratio, which was added simultaneously with a solution of $NH_4OH$ (10 %) into a beaker containing 300 mL of distilled water under constant stirring. This process was carried out in a peristaltic pump, keeping the pH at 9.2. The resulting system was heated at 90 °C for two hours, until reaching a pH of 8.3. This stage was carried out to eliminate the excess $NH_4OH$, decompose the blue hexamine-nickel cation $[Ni\ (NH_3)_6]^{2+}$, and precipitate the green nickel hydroxide $[Ni(OH)_2]$.

The initial precipitation process at pH of 9.2 was carried out to precipitate the aluminum hydroxide or oxyhydroxides and part of the nickel hydroxide while keeping part of the nickel in a soluble state, which subsequently precipitated on the aluminum compounds due to a pH decrease to 8.3 and through the decomposition of the blue nickel complex. The precipitate formed was filtered off under vacuum, dried at 80 °C for 24 hours, and calcined at 500 or 750 °C under an airflow of 100 mL $min^{-1}$ for 4 h.

The preparation of solids based on nickel-zinc-aluminum (Ni-Zn-Al) was similar to that used for the synthesis of materials based on Ni-Al, differing in the addition of $Zn(NO_3)_2$ $6H_2O$ during the initial mixing process.

Through this methodology, solids based on nickel-aluminum with a Ni/Al=0.5 molar ratio (solids A05-500 and A05-750) and solids based on nickel-zinc-aluminum with Ni/Zn molar ratios of 0.5 (solids AZ05-500 and AZ05-750), 1.0 (solids AZ10-500 and AZ10-750), and 1.5 (solids AZ15-500 and AZ15-750), whereby numbers 500 and 750, in the identification codes of the solids denote employed calcination temperatures.

### 2.2. Material characterization

Calcined materials were characterized using energy-dispersive X-ray spectroscopy (EDX), mid-infrared spectrometry with Fourier transform (FTIR), measurement of the specific surface area by BET method, X-ray diffraction (XRD), and temperature programmed reduction (TPR) analyses.

The EDX technique was used for metal determination in the compound solids. The analyses were carried out in a Shimadzu equipment model EDX-700HS, using the Al K$\alpha$ emission bands (1.48 KeV), Ni K$\alpha$ (7.97 KeV) and Zn K$\alpha$ (9.57 KeV).

FTIR analyses were performed in a Perkin Elmer equipment, model Spectrum One, in 4000-400 $cm^{-1}$ region in transmission mode. Prior to this analysis, all samples were previously mixed with potassium bromide salt at a 1:100 ratio and analyzed in the interval of 4000-400 $cm^{-1}$ with a resolution of 2 $cm^{-1}$.

XRD analyses were performed in a Shimadzu XDR-600 model, in the range 10-80 (2θ degrees), using Cu Kα radiation (1.5460 Å), generated at 40 kV and 30 mA.

The specific surface area was determined by adsorption of nitrogen at 196.15 °C and applying the BET method, using a Micromeritics ASAP 2010 instrument.

TPR analyses were carried out in a Micromeritics model TPD/TPR 2900 Analyzer, equipped with a thermal conductivity detector (TCD), using a heat-increase rate of 5 °C/min, from 30 to 1000 °C, employing a mixture consisting of 5 % $H_2$ and 95 % $N_2$ as reducing agent. The deconvolution and statistical analysis of the reduction peaks obtained from TPR were performed using a Gaussian model and plotted with the Origin 2018 software.

### 2.3. Catalytic evaluation

The solids were evaluated as catalysts in the WGS reaction at 260 ºC and 1 atm, using a flow of 150 mL/min of a mixture containing: carbon monoxide (3%), carbon dioxide (15%), nitrogen (22%), hydrogen (60%), and a relationship of mixture/water vapor of 0.8. All materials were previously reduced in situ in a tubular microreactor at 420 ºC, using a flow of 50 ml/min of $H_2$ for 1 h. The products of the reaction were quantified with a Thermo Finnigan chromatograph, model GC 2000, equipped with a packed column and a molecular sieve column, as well as TCD and FID detectors.

A temperature of 420 °C was chosen for the TPR analyses whereby NiO reduction that does not interact with the Al2O3-based support commences, while the reduction of similar NiO particles finished in ZnO/Al2O3-based supports. Reductions also took place at temperatures of 450 and 500 °C, but this led to less active solids for the WGS reaction, so the TPR evaluation focused on materials reduced at 420 °C only.

## 3. Results and Discussion

EDX results, shown in **Table 1**, indicate that the Ni/Al and Ni/Zn molar ratios are close to that projected during the synthesis process, which did not experience variation above 10% in the composition of the calcined materials.

**Table 1.** Ni/Al and Ni/Zn molar ratios determined by EDX in calcined materials.

| SAMPLE | Ni/Al MOLAR RATIO | NI/Zn MOLAR RATIO |
|---|---|---|
| A05-500 | 0.49 | --- |
| A05-750 | 0.52 | --- |
| AZ05-500 | 0.55 | 0.55 |
| AZ05-750 | 0.54 | 0.55 |
| AZ10-500 | 0.49 | 1.07 |
| AZ10-750 | 0.53 | 1.10 |
| AZ15-500 | 0.48 | 1.52 |
| AZ15-750 | 0.49 | 1.52 |

The FTIR spectra of solids A05-500 and A05-750 revealed a broad band around 3400 $cm^{-1}$, caused by the stretching mode of the OH bond of the physisorbed water molecules. This phenomenon also gave rise to a sharp band at 635 $cm^{-1}$ related to the HOH angle deformation vibrational mode. [27]. A band related to Al3+ ions of transition aluminas, located in tetrahedral and octahedral positions, was also observed at 800 cm-1. Furthermore, bands attributable to the presence of nickel aluminate (NiAl2O4) were found at 730 and 500 cm-1 [27,28,29,30] (**Figure 1**).

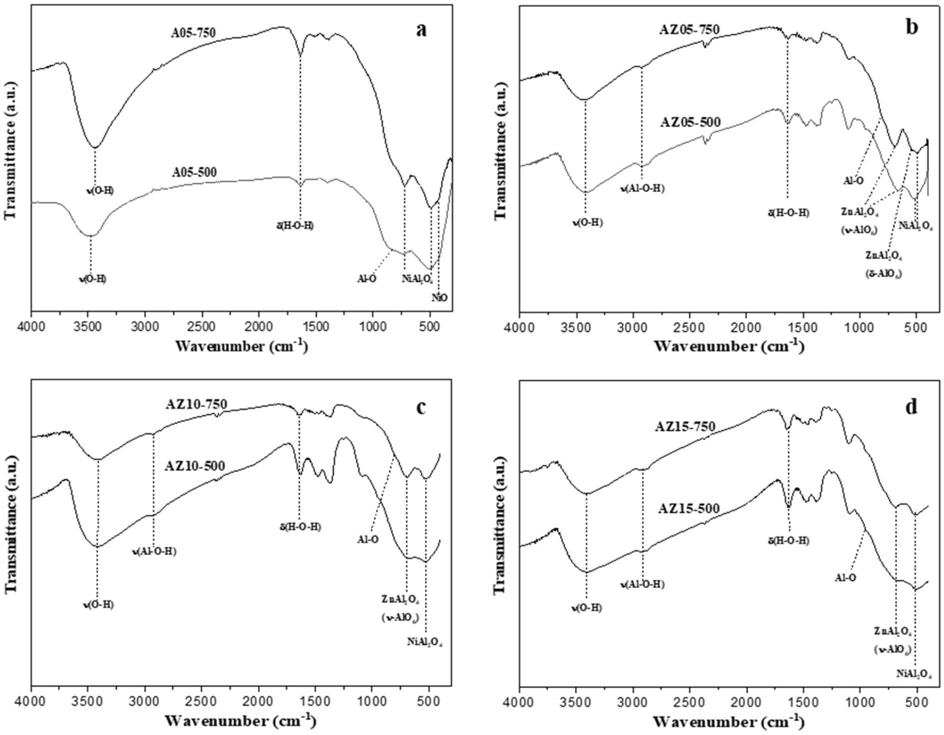

**Figure 1.** FTIR spectra of calcined solids at 500 and 750 °C, based on Ni-Al with Ni/Al = 0.5 ratio (a), and calcined solids based on Ni-Zn-Al keeping a constant Ni/Al = 0.5 ratio and varying the Ni/Zn ratios in the values of 0.5 (b), 1.0 (c) and 1.5 (d).

Physisorbed water molecules also formed bands in the zinc-containing materials. Those calcined at 500 °C exhibited bands at 660 and 500 $cm^{-1}$, which originated from the overlaying of bands associated with nickel aluminate and zinc aluminate ($ZnAl_2O_4$) [31]. In the solids prepared at 750 °C, bands were observed at 691, 536 and 495 $cm^{-1}$, associated with the presence of $ZnAl_2O_4$ (Zn-O-Al, 698.6 $cm^{-1}$), $\gamma$-alumina (vibration of the Al-O bond in tetrahedral positions of the spinel-type structure, 540 $cm^{-1}$) and $NiAl_2O_4$ (Ni-O-Al, 500 $cm^{-1}$) [30, 31].

The X-ray diffractograms of the calcined nickel and aluminum-based solids are shown in **Figure 2**, depicting phases corresponding to NiO and peaks attributable to $Ni_2Al_2O_4$. The latter were likely formed by the solid-state reaction between NiO and aluminum oxides present in the materials. Regarding the width and symmetry of the peaks corresponding to NiO, no significant differences were observed. The average size particle, calculated with the Scherrer equation and the crystallographic plane (*0 0 2*) of NiO was approximately 14 nm for the two solids. Additionally, the *a* parameters of cells, calculated with the Bragg equation and the (*0 0 2*) plane of the NiO phase, were 4.15 Å for A05-500 and 4.16 Å for A05-750, which are values below those recorded by the NiO reference sample (4.17 Å). This reference was prepared at 500 °C in conditions similar to those used to synthesize bimetal and trimetal solids. These results may be due to the presence of $Al^{3+}$ cations (0.53 Å) in the cubic structure of NiO (0.69 Å for $Ni^{2+}$), which causes a decrease in the cell parameter due to the lower ionic radius of aluminum.

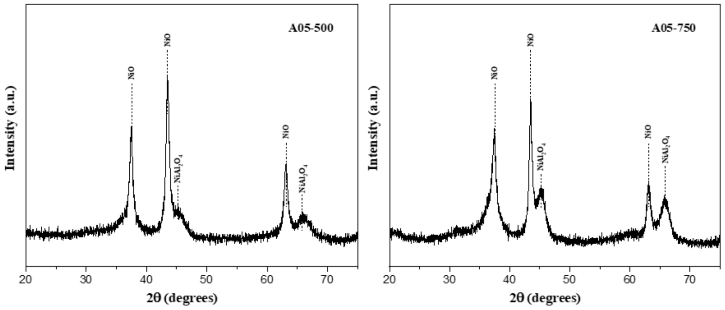

**Figure 2.** X-ray diffractograms (XRD) of solids constituted by Ni-Al with Ni/Al = 0.5 ratio and calcined at 500 and 750 ºC.

In these materials, the calcination temperature did not lead to any drastic differences in textural parameters, such as specific surface area with values of 159 $m^2/g$ (A05-500) and 132 $m^2/g$ (A05-750), indicating that the temperature and the increase in nickel aluminate content did not lead to considerable sintering effects.

The X-ray diffractograms of the nickel-zinc-aluminum-based solids are shown in **Figure 3**. In all materials, the NiO, $NiAl_2O_4$ and $ZnAl_2O_4$ phases were identified, while ZnO was only detected in the AZ05-500 material. The symmetry of the peaks decreased in the solids at lower zinc content, and the $NiAl_2O_4$ species primarily occurred in the AZ15-500 material. The broader peaks in materials with lower zinc content were caused by the presence of spinel-type structures, which occur in aluminates and transitional aluminas [1,2,32,33,34].

The samples prepared at 750 °C exhibited narrower and symmetrical diffraction peaks, several of which were attributable to $ZnAl_2O_4$ and, to a lesser extent, to $NiAl_2O_4$, being the result of reactions between NiO and ZnO with aluminum-based species. In these materials, due to the shape of the peaks, it was possible to determine the *a* cell parameter of NiO, thus coming across values of 4.19 Å (AZ05-750), 4.19 Å (AZ10-750), and 4.17 Å (AZ15-750), suggesting that $Zn^{2+}$ cations (0.74 Å) were likely incorporated into the cubic lattice of NiO, inducing an effect opposite to that produced by $Al^{3+}$ cations, due to their greater cationic radius [35].

As for the materials prepared at 500 °C: AZ05-500 (108 $m^2/g$), AZ10-500 (143 $m^2/g$), and AZ15-500 (155 $m^2/g$), the one with the highest zinc content showed the lowest specific surface area, being attributable to its own share of ZnO. Additionally, solids AZ10-500 and AZ15-500 showed broader diffraction peaks, allowing us to infer that, in these materials, the particles that make up such materials are smaller than those present in the AZ05-500 sample, which also contributes to higher values of the specific surface area. The decrease in the specific surface area, due to

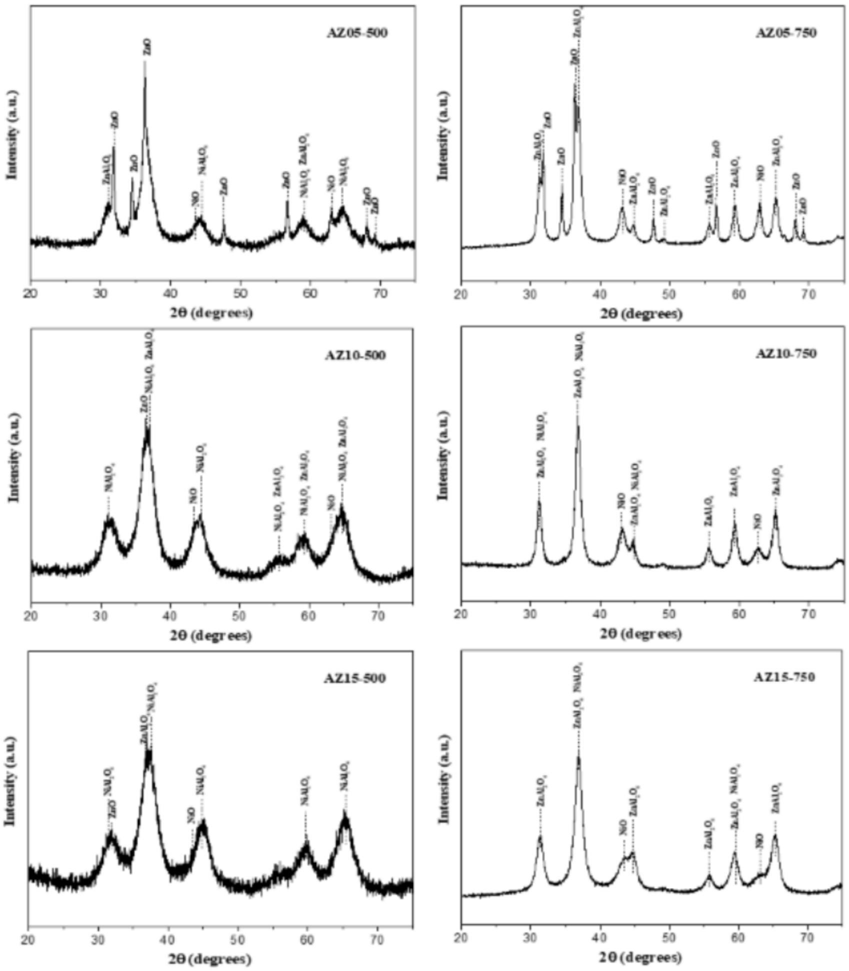

**Figure 3.** X-ray diffractograms (XRD) of solids constituted by Ni-Zn-Al with Ni/Al = 0.5 and Ni/Zn = 0.5, 1.0 and 1.5 ratios, calcined at 500 °C and 750 °C.

the presence of the ZnO, $NiAl_2O_4$ and $ZnAl_2O_4$ phases and by the sintering effect induced by the higher calcination temperature, was more evident in the AZ05-750 (48 $m^2/g$), AZ10-750 (72 $m^2/g$), and AZ15-750 (92 $m^2/g$) materials, where we observed that the increase in the zinc content lowered the value of this textural parameter [36].

**Figure 4** shows the TPR curves of the Ni-Al and Ni-Zn-Al-based materials, depicting several peaks, from deconvolution processes in the graphs, which indicate different types of NiO particles in the solids. In the TPR curves of the nickel-aluminum-based solids, a peak was observed at temperatures below 300 °C in the A05-500 material, which is indicative of the presence of NiO particles that do not interact with the aluminum oxide-based support [37,38,39].

these materials, two peaks were recorded between 400 and 600 °C, which are associated with NiO particles located on the surface of the support with weak and intermediate interactions. Next, peaks attributable to NiO units submerged in the volume of the support (~ 800 °C) were observed, which require the diffusion of hydrogen through the pores or cavities in the materials to be reduced. The peaks recorded at the highest temperatures may also be related to the reduction of NiO with the presence of $Al^{3+}$ in the crystal cubic lattice [40, 41].

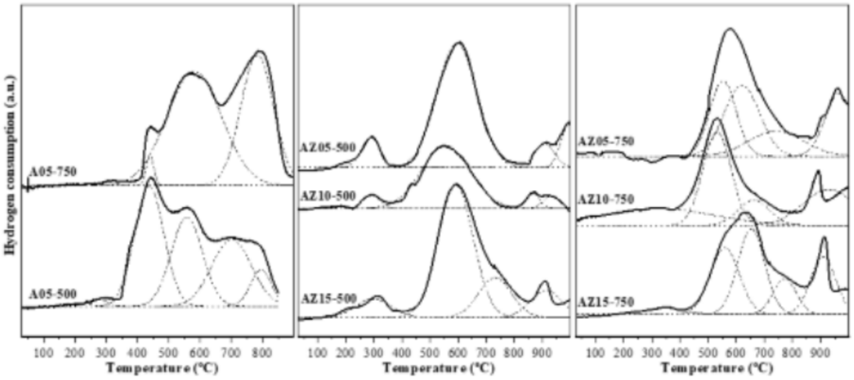

**Figure 4.** Temperature-programmed reduction (TPR) curves of solids constituted by Ni-Al and Ni-Zn-Al, calcined at 500 °C and 750 °C.

**Figure 5** shows that the highest hydrogen consumption for sample A05-500 occurs between 400 and 600 °C, indicating that most of the NiO is located on the surface of the solid, while, for material A05 -750, the high hydrogen consumption at temperatures close to 800 °C is associated with the reduction of NiO submerged in the support and at phases such as $NiAl_2O_4$ detected by XRD [37, 38].

Solids containing zinc and calcined at 500 °C originated a reduction peak at temperatures close to 300 °C (see Figure 4), indicating the presence of NiO, which is not interacting with the support: According to **??**, in these materials, this type of NiO particles is higher than that recorded by material A05-500, revealing that the presence of zinc partially preventing the interaction between NiO units and the aluminum oxide-based support. Only the AZ10-500 material exhibited NiO in a weak interaction with the support [2, 40, 42].

Zinc does not completely prevent the interaction between nickel species and the support, whereby reduction peaks were observed in such materials at temperatures close to 600 °C. This is attributable to NiO in intermediate interaction with the support, as illustrated in **??**. Only the AZ15-500 sample exhibited NiO in strong interaction with the support, showing a peak at 750 °C. All these materials recorded hydrogen consumption at temperatures above 850 °C, which confirms the presence of $NiAl_2O_4$ [37, 38].

The record of reduction peaks at temperatures between 340 and 380 °C for AZ10-750 and AZ15-750 (Figure 4 and Figure 7) indicates that zinc also contributes within materials calcined at 750 °C with the presence of NiO particles that do not interact with the support. However, the degree of interaction of NiO with the support is stronger in these materials than that recorded by the solids synthesized at 500 °C, being the reduction peaks displaced at higher temperatures.

The complete reduction of the NiO particles requires the diffusion of hydrogen through the previously reduced surface, thus forming $Ni^0$ nuclei that grow to occupy the entire volume of the particles [11], which, in the case of solids prepared at 750 °C, requires higher temperatures or more time because the particles in such materials have larger dimensions due to the effect of sintering generated by calcination at higher temperatures. This fact is inferred by the lower values of specific surface area and by the narrowest X-ray diffraction peaks. Additionally, the synthesis at 750 °C led to the formation of nickel aluminate ($NiAl_2O_4$), which, in turn, led to the depletion of over 20% of the necessary hydrogen required to reduce the nickel present in the samples.

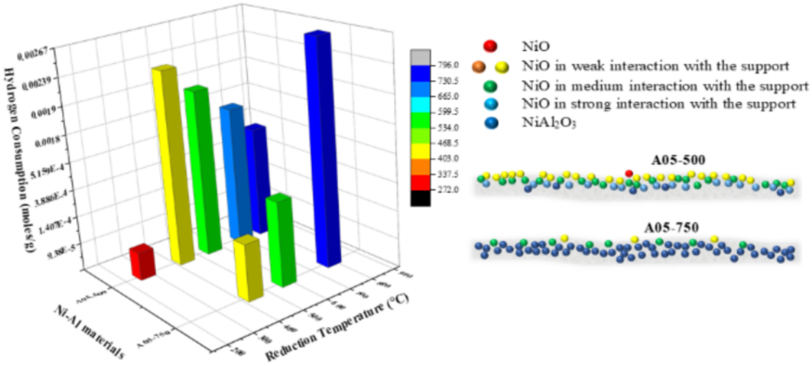

**Figure 5.** Hydrogen ($H_2$) consumption was calculated as the deconvolution of the peaks recorded by TPR for solids A05-500 and A05-750. The schemes located on the right side represent the percentage of NiO and $NiAl_2O_4$ particles present in solids.

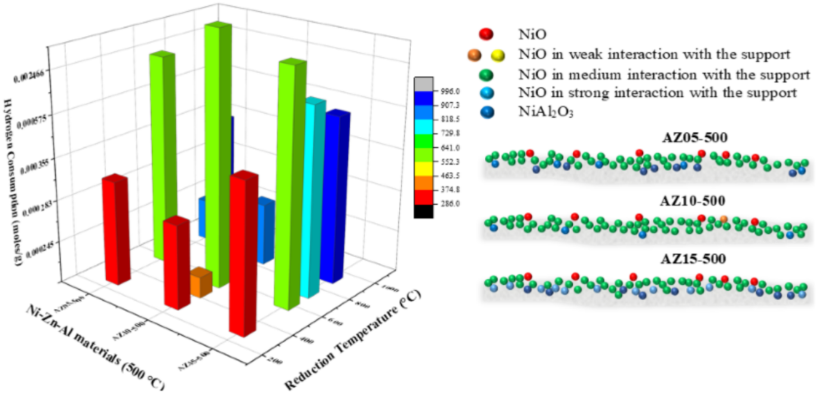

**Figure 6.** Hydrogen ($H_2$) consumption is calculated as the deconvolution of the peaks recorded by TPR for solids AZ05-500, AZ10-500, and AZ15-500. The schemes located on the right side represent the percentage of NiO and $NiAl_2O_4$ particles present in solids.

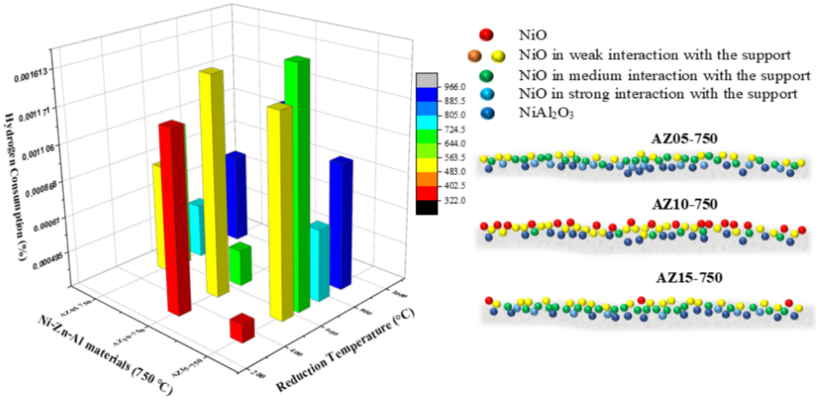

**Figure 7.** Hydrogen ($H_2$) consumption was calculated by the deconvolution of the peaks recorded by TPR for solids AZ05-750, AZ10-750, and AZ15-750. The schemes located on the right side represent the percentage of NiO and $NiAl_2O_4$ particles present in solids.

The diagrams on the right side of Figures 5-7 simulate the particle agglomerates of the nickel phases present in the solids. The presence of NiO particles located on the surface of the materials, which do not interact with them, causes for reduction peaks similar to those recorded by pure NiO. These diagrams also show NiO particles in locations close to the surface of solids, which, depending on the degree of immersion in the volume of the materials, can make for reduction peaks between ~ 330 and 730 °C due to weak, intermediate or strong interactions with the aluminum oxide-based support or species such as ZnO. Finally, it has been observed that, in the materials prepared at 750 °C, there are also $Ni_2O_4$ particles that were produced through solid state reactions between oxygenated nickel and aluminum compounds, which is reduced at temperatures greater than 850 °C [22].

The reduction temperatures recorded in this study differ from those recorded by Scheffert and collaborators [16], due to the differences in the synthesis methods used, since the solids used as reference were obtained by impregnation processes in alumina, whereas in Scheffert et al's work, nickel, zinc and aluminum oxides were produced in solids within which the distribution of the precursors was homogeneously split through the volume of the materials before the calcination process at 500 or 750 °C.

WGS catalysis reaction assessment results are shown in **Figure 8**. The materials assessed were reduced to 420 °C.

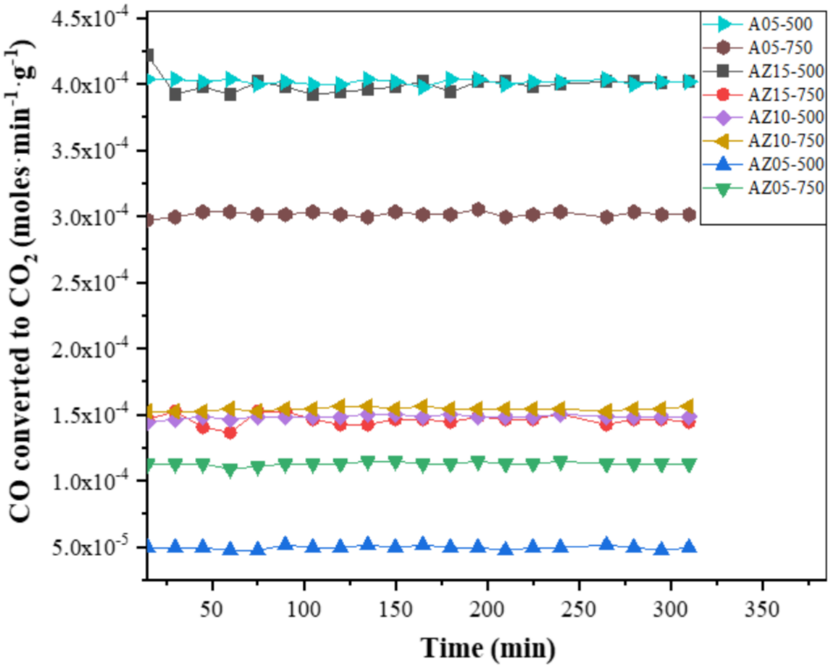

**Figure 8.** Conversion of carbon monoxide by WGS reaction of catalysts reduced *in situ* at 420 °C.

Nickel and aluminum-based catalysts were active for the reaction, with the A05-500 solid being the most active, being attributed to the higher content of $Ni^0$ present in this material, as evidenced by the larger area and intensity of the diffraction peaks of $Ni^0$ in relation to NiO, when compared to those recorded by the A05-750 material after catalytic evaluation (**Figure 9**). These results are consistent with the type of NiO particles that can be reduced at 420 °C, as shown in Figure 5, in which the A05-500 catalyst containing NiO, did not interact with the support nor did with the large number of particles of this oxide, which interact weakly with the support. Additionally, the A05-500 material (150 $m^2$/g) displayed, after the catalytic evaluation, a higher specific surface area than the A05-750 material (130 $m^2$/ g). Regarding selectivity, during the catalytic evaluation, in addition to hydrogen, methane production was observed at levels of 5% for A05-500 and 4% for A05-750.

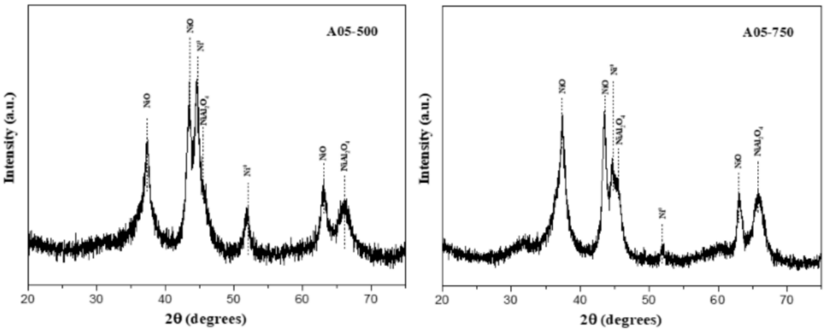

**Figure 9.** X-ray diffractograms (XRD) of spent catalysts constituted by Ni-Al with Ni/Al = 0.5 ratio and calcined at 500 and 750 ºC.

The presence of zinc led to a catalyst with 100% selectivity for the WGS reaction. Among the materials prepared at 500 °C, sample AZ15-500 showed the highest conversion rate, with values close to those obtained with A05-500. Furthermore, the increase in zinc led to a decrease in the surface area of the spent catalysts (AZ15-500, 148 $m^2$/g; AZ10-500, 133 $m^2$/g; AZ05-500, 107 $m^2$/g) and to a lower activity for the WGS reaction, where AZ05-500 was the least active material. The diffractograms of the materials used (**Figure 10**) showed profiles similar to those originated by the solids before the catalytic evaluation, with wide and asymmetric peaks being reported, which hinders the identification of metallic nickel among all materials.

The catalytic activity recorded by the solids is attributed to the metallic nickel that occurred during the *in situ* reduction, whose formation is possible, as shown in Figs. 6 and 7, in which we observed that $Ni^0$ can be obtained at 420 °C from NiO in a low or weak interaction with the support. Regarding the catalysts prepared at 750 °C, the most active ones were AZ15-750 and AZ10-750, with conversion rates similar and close to those recorded by sample AZ10-500. These materials did not show diffraction peaks attributable to metallic nickel after being used; however, TPR results indicate that $Ni^0$ formation was possible under the reduction conditions used before catalytic evaluation, which explains its activity. Sample AZ05-750 showed activity because its first reduction peak started at temperatures close to 420 °C, even when the presence of NiO without surface interaction was not evident.

## 4. Conclusions

Traditional analysis techniques allow the identification of nickel oxide supported on aluminum oxides. However, when the support shows amorphous structures, the identification of NiO is difficult. In this regard, the TPR technique led to the confirmation of NiO presence in all materials and offered information that revealed the types of NiO particles in the materials, as well as the degree of interaction between the oxide studied and the support based on aluminum oxide and zinc. In calcined materials, NiO that does not interact with the support was detected, and particles from

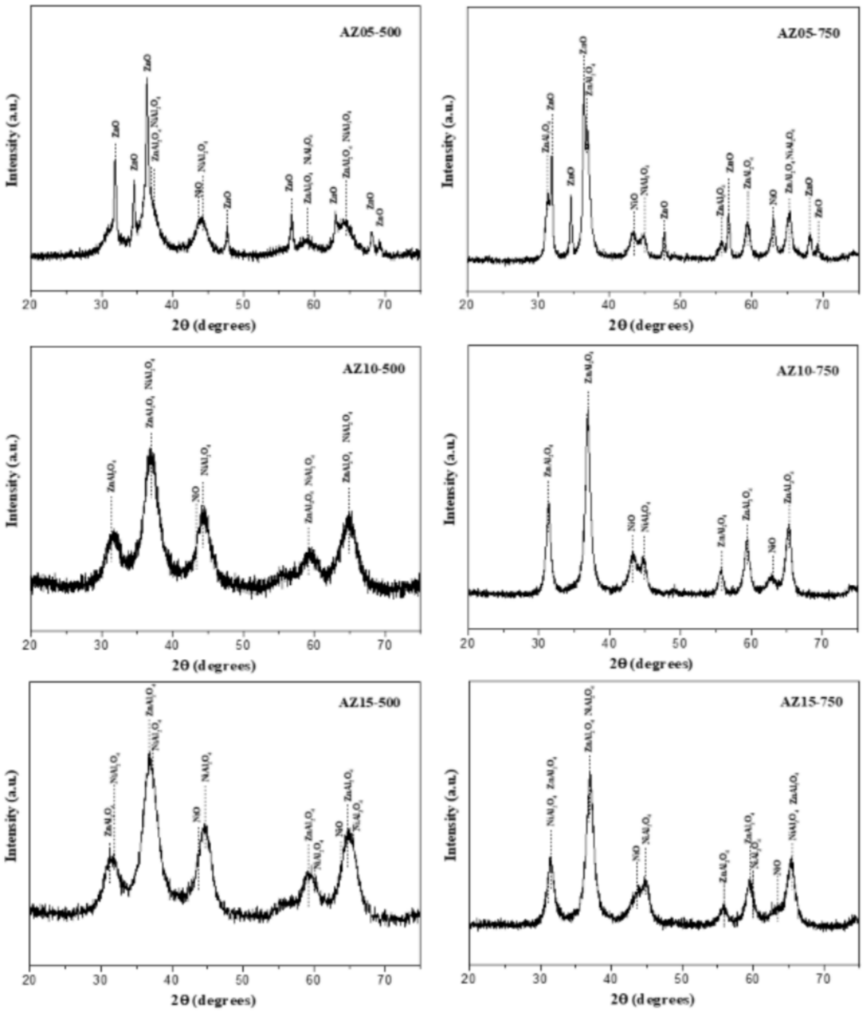

**Figure 10.** X-ray diffractograms (XRD) of spent catalysts constituted by Ni-Zn-Al with Ni/Al = 0.5 and Ni/Zn = 0.5, 1.0 and 1.5 ratios, calcined at 500 °C and 750 °C.

this oxide submerged near its surface were observed. In the case of materials prepared at higher temperatures, the degree of interaction rises, with nickel aluminate particles being detected. All catalysts were active for the WGS reaction. The presence of zinc led to increased selectivity but decreased specific surface area and activity in most cases. The AZ15-500 material was the most effective because it presented high activity and 100% of selectivity towards the WGS reaction.

## 5. Acknowledgements

The authors acknowledge the financial support of the University of Cartagena, SENA, and CNPq.

### Conflict of interest

The authors declare that they have no conflict of interest.

## References

[1] Meza E, Faro A, de-Freitas T, Assaf J, Rangel M. A comparison between copper and nickel-based catalysts obtained from hydrotalcite-like precursors for WGSR, *Catalysis Today*, 171: 290-296, 2011. doi: 10.1016/j.cattod.2011.03.082

[2] Meza-Fuentes E, Cadete-Santos F, Prakash S, Costa-Faro A, de Freitas-Silva T, Mansur-Assaf J, Rangel M. The effect of metal content on nickel-based catalysts obtained from hydrotalcites for WGSR in one step, *International Journal of Hydrogen Energy*, 39: 1-14, 2014. doi: 10.1016/j.ijhydene.2013.10.114

[3] Sewell GS, Van-Steen E, O'Connor CT. Use of TPR/TPO for characterization of supported cobalt catalysts, *Catalysis Letter*, 37: 255-260, 1996. doi:10.1007/BF00807763

[4] Li P, Chen Y, Zhang C, Huang B, Liu X, Liu T, Jiang Z, Li C. Highly selective hydrodesulfurization of gasoline on unsupported Co-Mo sulfide catalysts: Effect of $MoS_2$ morphology, *Applied Catalysis. A-General*, 533: 99-108, 2017. doi: 10.1016/j.apcata.2017.01.009

[5] Scheffer B, Dekker NJ, Mangnus PJ, Moulijn JA. A temperature-programmed reduction study of sulfided Co-Mo/$Al_2O_3$ hydrodesulfurization catalysts. *Journal of Catalysis*. 121: 31-46, 1990. doi: 10.1016/0021-9517(90)90214-5

[6] Mahieu C, Puzenat E, Geantet C, Cardenas L, Afanasiev P. Titania-Supported transition metals sulfides as photocatalysts for hydrogen production from propan-2-ol and methanol, *International Journal of Hydrogen Energy*, 44: 18038-18049, 2019. doi:10.1016/j.ijhydene.2019.05.080

[7] Shimoda N, Koide N, Kasahara M, Mukoyama T, Satokawa S. Development of oxide-supported nickel-based catalysts for catalytic decomposition of dimethyl sulfide, *Fuel*, 232: 485-494, 2018. doi:10.1016/j.fuel.2018.06.009

[8] Jiang Z, Liao X, Zhao Y. Comparative study of the dry reforming of methane on fluidised aerogel and xerogel Ni/$Al_2O_3$ catalysts. *Applied Petrochemical Research*. 3: 91-99, 2013. doi:10.1007/s13203-013-0035-9

[9] Touahra F, Sehailia M, Ketir W, Bachari K, Chebout R, Trari M, Cherifi O, Halliche D. Effect of the Ni/Al ratio of hydrotalcite-type catalysts on their performance in the methane dry reforming process. *Applied Petrochemical Research*, 6: 1-13, 2016. doi:10.1007/s13203-015-0109-y

[10] Navarro MV, Plou J, López JM, Grasa G, Murillo R. Effect of oxidation-reduction cycles on steam-methane reforming kinetics over a nickel-based catalyst. *International Journal of Hydrogen Energy*, 44: 12617-12627, 2019. doi:10.1016/j.ijhydene.2018.12.056

[11] Jankovic B, Adnadevic B, Mentus S. The kinetic study of temperature-programmed reduction of nickel oxide in hydrogen atmosphere. *Chemical Engineering Science,* 63: 567-575, 2008. doi:10.1016/j.ces.2007.09.043

[12] Berrocal G, da-Silva A, Assaf J, Albornoz A, Rangel MC. Novel supports for nickel-based catalysts for the partial oxidation of methane, *Catalysis Today*. 149: 240-247, 2010. doi:10.1016/j.cattod.2009.06.005

[13] Ma Q, Guo L, Fang Y, Li H, Zhang J, Zhao T, Yang G, Yoneyama Y, Tsubaki N. Combined methane dry reforming and methane partial oxidization for syngas production over high dispersion Ni based mesoporous catalyst, *Fuel Processing Technology*, 188: 98-104, 2019. doi:10.1016/j.fuproc.2019.02.013

[14] Di Giuliano A, Gallucci K, Foscolo PU, Courson C. Effect of Ni precursor salts on Ni-mayenite catalysts for steam methane reforming and on Ni-CaO-mayenite materials for sorption enhanced steam methane reforming. *International Journal of Hydrogen Energy*, 44:6461-6480, 2019. doi:10.1016/j.ijhydene.2019.01.131

[15] Pashchenko D. Experimental investigation of synthesis gas production by methane reforming with flue gas over a NiO-$Al_2O_3$ catalyst: Reforming characteristics and pressure drop. *International Journal of Hydrogen Energy,* 44:7073-7082, 2019. doi:10.1016/j.ijhydene.2019.01.250

[16] Scheffer B, Molhoek P, Moulijn J. Temperature-Programmed Reduction of $NiOWO_3/Al_2O_3$ Hydrodesulphurization Catalysts. *Applied Catalysis*, 46: 11-30, 1989. doi:10.1016/S0166-9834(00)81391-3

[17] Mile B, Stirling D, Zammitt MA, Lovell A, Webb M. TPR studies of the effects of preparation conditions on supported nickel catalysts. *Journal of Molecular Catalysis*, 62: 179-198, 1990. doi:10.1016/0304-5102(90)85212-Z

[18] Li C, Chen Y. Temperature-programmed-reduction studies of nickel oxide/alumina catalysts: effects of the preparation method. *Thermochimica Acta*, 256:457-465, 1995. doi:10.1016/0040-6031(94)02177-P

[19] Zhou Z, Han L, Bollas G. Kinetics of NiO reduction by H2 and Ni oxidation at conditions relevant to chemical-looping combustion and reforming. *International Journal of Hydrogen Energy*, 39: 8535-8556, 2014. doi:10.1016/j.ijhydene.2014.03.161

[20] Wang CB, Gau GY, Gau SJ, Tang CW, Bi JL. Preparation and characterization of nanosized nickel oxide. *Catalysis Letters* 101:241-247, 2005. doi:10.1007/s10562-005-4899-x

[21] Jafarbegloo M, Tarlani A, Mesbah W, Muzart J, Sahebdelfar S. NiO–MgO solid solution prepared by sol–gel method as precursor for Ni/MgO methane dry reforming catalyst: effect of calcination temperature on catalytic performance. *Catalysis Letter*, 146:238-248, 2016. doi:10.1007/s10562-015-1638-9

[22] Farahani MD, Valand J, Mahomed AS, Friedrich HB. A Comparative Study of NiO/$Al_2O_3$ Catalysts Prepared by Different Combustion Techniques for Octanal Hydrogenation. *Catalysis Letter*. 146: 2441-2449, 2016. doi:10.1007/s10562-016-1858-7

[23] Delgado D, Sanchís R, Cecilia JA, Rodríguez-Castellón E, Caballero A, Solsona B, López Nieto JM. Support effects on NiO-based catalysts for the oxidative dehydrogenation (ODH) of ethane. *Catalysis Today*. 333: 10-16, 2019. doi:10.1016/j.cattod.2018.07.010

[24] Qin H, Guo C, Wu Y, Zhang J (2014) Effect of $La_2O_3$ promoter on NiO/$Al_2O_3$ catalyst in CO methanation. *Korean Journal of Chemical Engineering*, 31: 1168-1173, 2014. doi:10.1007/s11814-014-0013-7

[25] Han SW, Jeong MG, Kim H, Seo HO, Kim YD. Use of NiO/$SiO_2$ catalysts for toluene total oxidation: Catalytic reaction at lower temperatures and repeated regeneration. *Chinese Journal of Catalysis*, 37: 1931-1940, 2016. doi:10.1016/S1872-2067(16)62514-7

[26] Fukudome K, Kanno A, Ikenaga N, Miyake T, Suzuki T. The oxidative dehydrogenation of propane over NiO–ZrO2 catalyst. *Catalysis Letter*, 141: 68-77, 2011. doi:10.1007/s10562-010-0461-6

[27] Jitianu M, Jitianu A, Zaharescu M, Crisan D, Rodica M. IR structural evidence of hydrotalcites derived oxidic forms. *Vibrational Spectroscopy*, 22: 75-86, 2002. doi:10.1016/S0924-2031(99)00067-3

[28] Milanović M, Obrenović Z, Stijepović I, Nikolić LM. Nanocrystalline boehmite obtained at room temperature. *Ceramics International,* 44: 12917–12920, 2018. doi:10.1016/j.ceramint.2018.04.103

[29] Li DY, Lin YS, Li YC, Shieh DL, Lin JL. Synthesis of mesoporous pseudoboehmite and alumina templated with 1-hexadecyl-2,3-dimethyl-imidazolium chloride. *Microporous and Mesoporous Materials*, 108: 276–282, 2008. doi:10.1016/j.micromeso.2007.04.009

[30] Liu C, Shih K, Gao Y, Li F, Wei L. Dechlorinating transformation of propachlor through nucleophilic substitution by dithionite on the surface of alumina. *Journal of Soils and Sediments*, 12: 724-733, 2012. doi:10.1007/s11368-012-0506-0

[31] Lu W, Lu G, Liu X, Guo G, Wang J, Guo Y. Effects of support and modifiers on catalytic performance of zinc oxide for hydrogenation of methyl benzoate to benzaldehyde. *Materials Chemistry and Physics*, 82: 120-127, 2003. doi:10.1016/S0254-0584(03)00207-4

[32] Gonçalves A, Costa M, Zhang L, Ciesielczyk F, Jaroniec M. One-pot synthesis of $MeAl_2O_4$ (Me = Ni, Co, or Cu) supported on $\gamma$-$Al_2O_3$ with ultralarge mesopores: Enhancing interfacial defects in $\gamma$-Al2O3 to facilitate the formation of spinel structures at lower temperatures. *Chemistry of Material*. 30: 436-446, 2018. doi:10.1021/acs.chemmater.7b04353

[33] Srinatha N, Satyanarayana S, Suriyamurthy N, Rudresh KJ, Suresh MR, Madhu A, Angadi B. New fuel governed combustion synthesis and improved luminescence in nanocrystalline $Cr^{3+}$ doped $ZnAl_2O_4$ particles. *Results in Optics*. 8: 100242, 2022. doi:10.1016/j.rio.2022.100242

[34] Fahoul Y, Zouheir M, Tanji K, Kherbeche A. Synthesis of a novel $ZnAl_2O_4$/CuS nanocomposite and its characterization for photocatalytic degradation of acid red 1 under UV illumination. *Journal of Alloys and Compounds,* 889: 161708, 2021. doi:10.1016/j.jallcom.2021.161708

[35] Meza E & Rangel M. Síntesis de catalizadores de Ni/ZnO/$Al_2O_3$ para la reacción WGS a través del estudio de las propiedades estructurales y catalíticas de Ni/ZnO y Ni/$Al_2O_3$. *Revista Colombiana de Química*, 40: 105-123, 2011. doi:10.15446/rev.colomb.quim

[36] Meza-Fuentes E, Rodriguez-Ruiz J, Solano-Polo C, Rangel MC, Faro A. Monitoring the structural and textural changes of Ni-Zn-Al hydrotalcites under heating. *Thermochimica Acta*. 687: 178594, 2020. doi:10.1016/j.tca.2020.178594

[37] Hoffer BW, Van-Langeveld AD, Janssens JP, Bonné RLC, Lok CM, Moulijn JA. Stability of highly dispersed Ni/$Al_2O_3$ catalysts: Effects of pretreatment. *Journal of Catalysis*, 192: 432-440, 2000. doi:10.1006/jcat.2000.2867

[38] Mangnus PJ, Bos A, Moulijn JÁ. Temperature-programmed reduction of oxidic and sulfidic alumina-supported NiO, $WO_3$, and NiO-$WO_3$ catalysts. *Journal of Catalysis*, 146: 437-448, 1994. doi:10.1006/jcat.1994.1081

[39] Ding C, Liu W, Wang J, Liu P, Zhang K, Gao X, Ding G, Liu S, Han Y, Ma X. One step synthesis of mesoporous NiO–$Al_2O_3$ catalyst for partial oxidation of methane to syngas: The role of calcination temperature. *Fuel,* 162: 148-154, 2015. doi:10.1016/j.fuel.2015.09.002

[40] Lundegaard LF, Tiruvalam RR, Tyrsted C, Carlsson A, Morales-Cano F, Ovesena CV. Migrating Al species hindering NiO reduction on Al containing catalyst carriers. *Catalysis Today*, 272: 25-31, 2016. doi:10.1016/j.cattod.2015.08.055

[41] Richardson JT, Twigg MV. Reduction of impregnated NiO/$\alpha$-$Al_2O_3$ association of $Al^{3+}$ ions with NiO. *Applied Catalysis A: General*. 167: 57-64, 1998. doi:10.1016/S0926-860X(97)00298-6

[42] Meza-Fuentes E, Rodriguez-Ruiz J, Rangel M. Characteristics of NiO present in solids obtained from hydrotalcites based on Ni/Al and Ni-Zn/Al. *DYNA*. 86: 58-65, 2019. doi:10.15446/dyna.v86n210.78559

## Estudio de los catalizadores NiO/$Al_2O_3$ y NiO/Zn-$Al_2O_3$ para la reacción de desplazamiento del gas de agua

**Resumen:** Los catalizadores basados en níquel son de gran importancia para la generación de hidrógeno a partir de gas natural, lo que hace necesario conocer las condiciones en las que el NiO/Al2O3 comercial se convierte en el catalizador Ni0/$Al_2O_3$. La Reducción Programada por Temperatura es una técnica ampliamente utilizada que permite identificar las condiciones de reducción de $Ni_2^+$ y los diferentes compuestos o tipos de partículas en las que este elemento está presente. En este trabajo, se estudió el tipo de partículas de óxido de níquel que ocurren en soportes basados en $Al_2O_3$ y ZnO-$Al_2O_3$ mediante diferentes técnicas, como espectroscopía de rayos X de dispersión de energía, FTIR, método BET, difracción de rayos X (XRD) y Reducción Programada por Temperatura (TPR). Los materiales fueron evaluados en la reacción de desplazamiento del gas de agua (WGS), y se estudió adicionalmente la influencia de las características de los materiales en la actividad catalítica. Los sólidos se prepararon a diferentes temperaturas y relaciones molares Ni/Zn. Los resultados mostraron la presencia de NiO en todos los materiales, así como la presencia de ZnO, $NiAl_2O_4$ y $ZnAl_2O_4$ en materiales preparados a temperaturas más altas. En todos los materiales calcinados a la temperatura más baja, se priorizó la formación de partículas de NiO que no interactuaban con los soportes. A medida que aumentaba la temperatura de calcinación, se formaron agregados de NiO que interactuaban en mayor medida con los soportes, detectándose aluminato de níquel en todos los materiales preparados a 750 °C. El zinc aumentó la selectividad, pero disminuyó el área superficial específica y la actividad mediante la reacción de WGS. El sólido etiquetado como AZ15-500 mostró una mayor actividad y selectividad, alcanzando valores del 100 % para la reacción de desplazamiento del gas de agua.

**Palabras Clave:** partículas de NiO; reducción programada por temperatura; efecto de la temperatura; catálisis; reacción de desplazamiento del gas de agua; producción de hidrógeno.

## Estudo dos catalisadores NiO/$Al_2O_3$ e NiO/Zn-$Al_2O_3$ para a reação de deslocamento água-gas

**Resumo:** Os catalisadores à base de níquel têm grande importância na geração de hidrogênio a partir de gás natural, o que torna necessário conhecer as condições em que o NiO/Al2O3 comercial se converte no catalisador Ni0/$Al_2O_3$. A Redução Programada por Temperatura é uma técnica amplamente utilizada que permite identificar as condições de redução de Ni2+ e os diferentes compostos ou tipos de partículas em que este elemento está presente. Neste trabalho, estudou-se o tipo de partículas de óxido de níquel que ocorrem em suportes à base de $Al_2O_3$ e ZnO-$Al_2O_3$ por meio de diferentes técnicas, como espectroscopia de raios-X por dispersão de energia, FTIR, método BET, difração de raios-X (XRD) e Redução Programada por Temperatura (TPR). Os materiais foram avaliados na reação de deslocamento água-gas (WGS), e foi estudada adicionalmente a influência das características dos materiais na atividade catalítica. Os sólidos foram preparados em diferentes temperaturas e relações molares Ni/Zn. Os resultados mostraram a presença de NiO em todos os materiais, assim como a presença de ZnO, $NiAl_2O_4$ e $ZnAl_2O_4$ em materiais preparados a temperaturas mais altas. Em todos os materiais calcinados à temperatura mais baixa, a formação de partículas de NiO que não interagiam com os suportes foi priorizada. À medida que a temperatura de calcinação aumentava, formavam-se agregados de NiO que interagiam em maior grau com os suportes, sendo detectado aluminato de níquel em todos os materiais preparados a 750 °C. O zinco aumentou a seletividade, mas reduziu a área superficial específica e a atividade por meio da reação WGS. O sólido rotulado como AZ15-500 mostrou maior atividade e seletividade, alcançando valores de 100% para a reação de deslocamento água-gas.

**Palavras-chave:** partículas de NiO, redução programada por temperatura, efeito da temperatura; catálise; reação de deslocamento água-gas; produção de hidrogênio.

**Edgardo Meza-Fuentes** Received the BSc. in Chemistry in 2001 from Universidad de Cartagena, Colombia, MSc. and PhD in Chemistry from Universidade Federal de Bahia, Brazil in 2006 and 2009, respectively. Currently, works as assistant professor at the Universidad de Cartagena and as director of the Group on Materials and Fuels Studies. His research interests include: heterogeneous catalysis, carbochemistry, chemometrics and environmental chemistry.

ORCID: 0000-0003-3725-8112

**Johana Rodriguez Ruiz** Received the BSc. in Chemistry in 2001 from Universidad de Cartagena, Colombia, and MSc. in Chemistry from Universidade Federal de Bahia, Brazil, in 2007. Currently, works as instructor at the Centro para la Industria Petroquímica-SENA, Colombia and as director of Group of Investigation in Processes of the Petrochemical Industry. His research interests include: oil analysis, synthesis and degradation of polymers, heterogeneous catalysis and environmental chemistry.

ORCID: 0000-0002-4263-4242

**Edinson Castellar Arroyo** Received the BSc. in Chemistry in 2017 from Universidad de Cartagena, Colombia, and MSc. in Chemistry from Universidad de Cartagena, Colombia, in 2023. His research interests include: synthesis and degradation of polymers, heterogeneous catalysis and environmental chemistry.

ORCID: 0000-0003-2181-3388

**Maria Rangel** Received the BSc. Eng in Chemical Engineering in 1979, MSc. in Chemistry in 1985, all of them from Universidad Federal de Bahía and PhD in Chemistry in 1991 from Universidade Estadual de Campinas, Brazil. He has done postdoctoral studies at Universidad Autónoma de Madrid, Spain and at the Centre National de la Recherche Scientifique. Additionally, he has worked as coordinator of graduate programs in chemistry at Universidade Federal de Bahia and acts as a guest editor in Catalysis Today. In the 1979-2016 period, he worked as a professor and researcher at Universidade Federal de Bahia. He is currently a full-time professor at Universidade Federal de Rio Grande do Sul, Brazil. His research interests include catalytic transformations of biomass, generation and purification of hydrogen; improving the quality of diesel and gasoline; production of clean fuels; generation of synthesis gas; fuel cells and advanced oxidative processes.

ORCID: 0000-0002-2497-9837

**Eduardo Espinosa Fuentes** Received the BSc. in Chemistry in 2004 from Universidad de Cartagena, Colombia, MSc. and PhD in Chemistry from Universidad de Puerto Rico, in 2010 and 2014, respectively. Currently, works as professor at the Universidad de la Costa, Barranquilla, Colombia. His research interests include: synthesis, characterization and detection of explosives, degradation of polymers, heterogeneous catalysis and environmental chemistry.

ORCID: 0000-0003-1653-5408